The Scientific Bulletin of VALAHIA University
MATERIALS and MECHANICS –Vol. 18, No. 19

DOI 10.2478/bsmm-2022-0013



DOUBLE-SUBSTITUTED CARBONATED HYDROXYAPATITES FOR FIR WOOD TREATMENT

Ramona Marina GRIGORESCU[1], Lorena IANCU[1*], Rodica-Mariana ION[1,2*], Madalina Elena DAVID[1,2], Elvira ALEXANDRESCU[1], Marius GHIUREA[1], Raluca Maria STIRBESCU[3]

[1] National Institute for Research and Development in Chemistry and Petrochemistry – ICECHIM, 202 Splaiul Independentei, 060021, Bucharest, Romania
[2] Valahia University from Targoviste, Doctoral School of Materials Engineering, 13 Aleea Sinaia, 13004 Targoviste, Romania
[3] Valahia University from Targoviste, Institute of Multidisciplinary Research for Science and Technology, Aleea Sinaia, 13004, Targoviste, Romania

Email: lorenna77ro@yahoo.com; rodica_ion2000@yahoo.co.uk

Abstract: The aim of the paper consist in the synthesis of double substituted carbonated hydroxyapatite using Zn^{2+} and Mg^{2+} ions in comparison with the previous obtained Sr-Zn-CHAp. Fourier transform infrared spectroscopy, X-ray diffraction, environmental scanning electron microscope (ESEM) coupled with EDS is used to highlight the presence of the metallic ions into the apatite structure. Both inorganic compounds are tested as consolidants for two types of fir wood, young and 30-years old samples. The consolidation efficiency is demonstrated by colorimetric analysis, mechanical tests and the specific methods for water absorption behavior. Stronger specimens, especially of young wood, with no significant color differences, more hygroscopic and with higher hysteresis index result after treatment. In conclusion, carbonated hydroxyapatite double substituted with zinc, magnesium and strontium ions can be used in wood preservation-conservation techniques.
Keywords: *Double substituted carbonated hydroxyapatites, wood treatments, artifacts conservation*

1. INTRODUCTION

The methodologies for the conservation and restoration of wood artefacts need a continuous development as this material is subjected to various factors regarding weathering, fungi and microorganism action, or fire degradation, so that history and culture can be passed on to the next generations [1].

Wood is and has been always intensively used in our everyday life for fuel and paper obtaining, construction industry, decorations including statues or icons, and furniture, etc. It is a porous and fibrous organic material, supporting thus a continuous degradation and deterioration [2-4]. Wood was and continues to be essential to human society and the researches in this area lead to an evolution from a simple and easy naturally found material to an engineering one with various characteristics for every application [5]. Its fibrous structure provides to items high strength, different color and densities, low weight, a relative durability [3, 6]. The main disadvantages of wood products are given by both the molecular structure of the main cell wall polymers and high content of hydroxyl groups (-OH) and consist in the susceptibility at microorganism attack, especially fungi, and instability in fluctuating moisture conditions when the material changes the conformational and dimensional stability. These actions affect the aesthetic value of items, their physical and resistance characteristics and structural integrity [2, 7, 8].

Most often, old wooden objects are severely affected by insects or fungi, having a high historical biological degradation. Improved mechanical stability to environmental degradation, hygroscopicity, etc. can result from the conservation-preservation-restoration procedures. Various methods to apply a consolidant were studied in time. Immersion can be easily used in lab studies, but it is not efficient on sites and for large objects and artifacts; poulticing is suitable to obtain a proper penetration depth of consolidant both in laboratory and real conditions; spraying can be used for obtaining homogenous coatings even on sites, but with a high consumption of consolidant and solvent vapors eliminated into the environment; brushing leads to a consistent treatment especially if a major attention is given to the control of all the applying parameters [9-13].

Nanotechnology and nanomaterials can be considered suitable for wood preservation. The small-sized nanoparticles can deeply penetrate and be uniform distributed though wood walls, and ensuring thus the surface modification for a high-performance products. Hydrophobic, abrasion, decay resistance and strengthened surfaces can be obtained by reducing the pores sizes that can absorb the water molecules and blocking the flow path of moisture inside wood [14].

Modifying wood items, native or artifacts, by applying nanotechnology, especially by a coating treatment, can lead to next-generation products with high performance and long-term service ability. The consolidant have to be chosen considering the required protection time, the appearance and the characteristics of the resulted coating [3].

There were developed various materials efficient in the preservation and conservation of cultural heritage objects. Among these solutions, hydroxyapatite (HAp) can be also considered as an useful consolidating agent for wood and other materials like paper or stone [15]. Despite that, it is known that HAp has a relative low mechanical resistance and a way to increase this characteristic consists in obtaining apatite materials having in their structure magnesium ions, silver, barium, zinc and copper [16-20]. Carbonated hydroxyapatite (CHAp) powder presents better homogeneity and consolidating efficacy, especially as nano sized [21]. The use of CHAp prevents the nanomaterial releasing in aqueous environment or in air, as can be observed for HAp or metallic nanoparticles.

A system based on gold hydroxyapatite (AuHAp) was tested on hazelnut wood samples and the efficiency on wooden artifacts preservation was demonstrated by morphologic, structural, chromatic, mechanical and permeability characterization. The AuHAp layer was uniform, covering the wood fibers and pores and thus improving the mechanical properties and hygroscopicity of both young and aged wood specimens [3]. The inclusion of specific metallic ions (for example Zn, Sr, Mg, etc.) can impart to the used coating antimicrobial properties.

The aim of this paper is to study the efficiency of two double substituted carbonated hydroxyapatites as consolidants for young and old wood specimens, by morphological, structural, colorimetric, and hygroscopic properties. The inorganic compounds contain zinc as main metallic ion and magnesium and strontium ions as the second path of calcium substitution. The synthesis method previous reported for Sr-Zn-CHAp [20] will be used for Mg-Zn-CHAp obtaining and, after its characterization, the wood samples will be treated by brushing with three different concentration of consolidant and tested.

2. MATERIALS AND METHODS

As wood samples, commercial young fir wood (YF) samples and 30-year-old fir wood specimens (30F) from an own collection were used. The specimen's dimensions were similar for the two types of wood, of about 3x3 cm for YF and 2x5 cm for 30F, Figure 1.

Double-substituted carbonated hydroxyapatite was synthetized according to [19, 20].

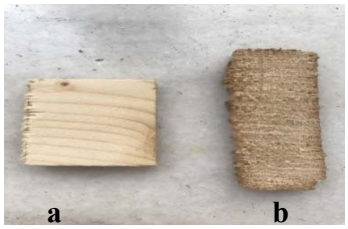

Figure 1. Wood specimens: a) young fir wood and (b) thirty-year-old fir wood

By comparison with Sr-Zn-CHAp, in case of Mg-Zn-CHAp, the used precursor were $Mg(NO_3)_2 \cdot 6H_2O$ and $Zn(NO_3)_2 \cdot 6H_2O$ considering that the metallic ions that can replace Ca^{2+} from the structure of CHAp.

In order to study the influence of the consolidate amount on the variation of wood properties, the samples were treated by brushing with the three suspensions, of 0.1 g/L, 0.25 g/L, and 0.5 g/L respectively from every powder.

3. CHARACTERIZATION METHODS

The similarities of Mg-Zn-CHAp compared with Sr-Zn-CHAp were evidenced by structural and morphological characterization.

The X-ray diffraction (XRD) pattern was achieved using with a Rigaku Ultima IV diffractometer (Rigaku, Tokyo, Japan) by applying a Cu Kα radiation with λ of 1.54 Å. The generator accelerating voltage the radiation was established at 40 kV. The emission current was of 200 mA. The 2θ range between 10º and 80º was scanned with a rate of 4º/min.

Fourier transform infrared spectroscopy (FTIR) has been performed with single-bounce diamond-attenuated total reflectance (ATR) using a Vertex 80 spectrometer (Bruker Optik GMBH, Germany), equipped with DRIFT accessory in the range of 4000–400 cm^{-1}.

The morphology of the inorganic consolidant was studied by environmental scanning electron microscopy (ESEM) with an FEI-Quanta 200 microscope incorporated with EDX module for spectrum imaging and profiling. The samples, without any covering, were tested in low vacuum mode.

The treated wood samples were analyzed in terms of colorimetric and mechanical properties, and also the water absorption characteristics were determined. The resistance of the treated samples compared to the control on the microbiological attack was evidenced.

The change in chromatic parameters after wood treatment was achieved using a CR-410 handheld chromameter (Konica Minolta, Tokyo, Japan). The CR-410 is perfectly suited for structured of rough samples, such as granulates, fabrics, wood, stones, bricks. The determinations in CIE L*a* b* system were made for both the control and the treated samples and the total color difference ΔE_{xfinal} was calculated according to EN 15886 [22] and ASTM 2244 [23], Equation (*1*).

$$\Delta E_{xfinal} = [\Delta L^2 + \Delta a^2 + \Delta b^2]^{1/2} \quad (1)$$

where, ΔL is the difference in lightness ($\Delta L = |L_{treated\ wood} - L_{control}|$), Δa is the chromatic deviation of the red-green coordinate ($\Delta a = |a_{treated\ wood} - a_{control}|$), and Δb is chromatic deviation of the yellow-blue coordinate ($\Delta b = |b_{treated\ wood} - b_{control}|$), changes calculated reported to the control samples.

The compressive strength expressed as the rebound number (Q) was obtained according to ASTM C805, using a Silver Schmidt Hammer Proceq test hammer, L model that has a 0.735 Nm impact energy. The strength range of the Silver Schmidt test hammer is from 10–100 N/mm^2. Ten measurements were performed on each specimen, and then their average was made. The strength was calculated using Equation (*2*).

$$Compressive\ strength = 2.77 * e^{0.048*Q} \quad (2)$$

Water absorption measurement is an easy laboratory process in order to evaluate the deterioration degree due to the environment humidity and to monitor the efficacy of conservation/preservation treatments. The total water absorbed by the material ca be calculated according to Formula (3) considering the weight of dried sample (W_1) and the weight of the sample immersed for 24h in distilled water (W_2).

$$\text{Water Absorption (\%)} = \frac{W2-W1}{W1} * 100 \quad (3)$$

Being a hygroscopic material, in environmental conditions, wood absorbs and desorbs moisture due to the hydroxyl groups from the cell walls. The wood dimensional stability and the durability in real conditions depend on the water sorption/desorption hysteresis. The test was achieved simultaneous for young and the 30-years old fir wood samples. The specimens were placed in a climatic chamber with controlled temperature and humidity. By maintaining 25 °C, the humidity was varied from 50% to 95% and the samples were weighted every 30 minutes.

For the sorption test, the wood items were dried at 105 °C until constant mass and then placed in the climatic chamber. The amount of moisture adsorbed into each specimen per unit surface area under the specific humidity value is expressed in the adsorption curve.

For the desorption test, the samples were saturated by immersion in water for 24 h and then calculated the loss in humidity under controlled conditions.
In both case, the kinetics of sorption-desorption processes resulted by plotting the humidity percent reported to time and fitting the curves. The hysteresis index (HI), in order to evaluate the specific structural changes, was calculated with the Equation (*4*).

$$HI = \frac{Msorption - Mdesorption}{Mdesorption} * 100 \quad (4)$$

where $M_{desorption}$ and $M_{sorption}$ are the sample mass of the at the desorption and sorption equilibrium at the same humidity value.

The samples were measured before and after the sorption and desorption test in order to evaluate the dimensional changes on specimens. Length, width, and thickness were precisely measured using a digital caliper.

4. RESULTS AND DISCUSSIONS

In the first step, the research was focused on the synthesis and characterization of Mg-Zn-CHAp in comparison with Sr-Zn-CHAp previous obtained, and then to study their effect on the wood characteristics.

FTIR spectrum of Mg-Zn-CHAp presented in Figure 2(*a*) evidenced the specific groups of apatite structure. The main domain where the specific peaks in 1500-400 cm^{-1} appear is shown as graph insertion. The presence of phosphate is given by the bands from 1011, 1025, 980, 964, and 946 cm^{-1}. The sharp band at 3574 cm^{-1} and the one from 630 cm^{-1} are assigned to vibrational stretching modes of the O-H group. Carbonate presence is sustained by the bands from 1120 and 1085 cm^{-1}, specific to nonstoichiometric apatite [24]. The inclusion of metallic ions into the structure can be evidenced by the peaks from the 600-400 cm^{-1} range.

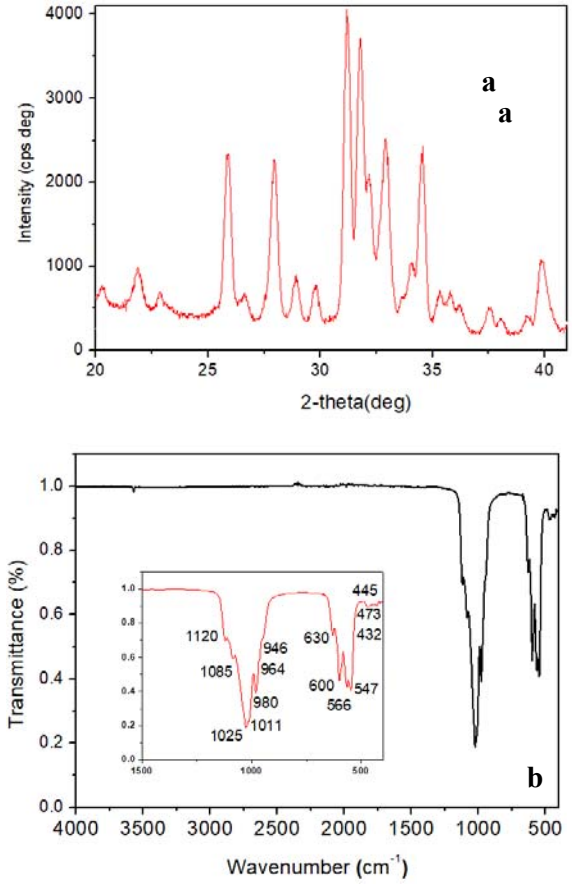

Figure 2. FTIR spectrum (*a*) and XRD diffractogram (*b*) for Mg-Zn-CHAp

The diffraction pattern of the Mg-Zn-CHAp is presented in Figure 2(*b*). The presence of metallic ions is evidenced by the peaks appeared at 20.29°, 26.55°,

29.78°, and the four peaks in the range between 35 and 38°, being confirmed the calcium substitution into CHAp lattice. [25]

By comparing the diffractogram with synthetic hydroxyapatite (ICDD 01-074-9780), similar structure can be observed. The main specific peak of apatite structure is given in Table 1.

The insertion of magnesium ions produces structural changes in apatite. The appearance of the peak from 31.2° proves the formation of β-tricalcium phosphate (TCP) structure at Mg-Zn-CHAp. The peak is specific to calcium-deficient apatites when hydroxyapatite is transformed to TCP [26]. Changes in d-spacing and crystallite size (L) calculated using the Scherrer's equation (*5*) could be observed (Table 1).

$$L = \frac{K \cdot \lambda}{\beta \cdot \cos\theta} \qquad (5)$$

where K is considered the shape factor (with a value of 0.9); λ is 1.54 Å); β is the full-width at half-maximum of the peak (radians); ɵ is the Bragg angle.

Table 1. The crystallite dimension of carbonated hydroxyapatite double substituted

Sr-Zn-CHAp [20]				Mg-Zn-CHAp				Miller index
2 θ, °	d, Å	β, (deg)	L, Å	2 θ, °	d, Å	β, (deg)	L, Å	
10.82	8.171	0.3725	238.05	10.83	8.162	0.367	217.41	(1,0,0)
16.92	5.236	0.4092	218.11	17.02	5.206	0.3826	209.93	(1,0,1)
21.75	4.083	0.3637	247.16	21.79	4.074	0.3777	214.22	(2,0,0)
25.80	3.451	0.3395	266.76	25.86	3.442	0.3322	245.39	(0,0,2)
27.80	3.207	0.4925	184.65	27.94	3.191	0.3663	223.46	(1,0,2)
28.86	3.091	0.3255	280.04	28.91	3.085	0.3362	243.99	(2,1,0)
31.73	2.818	0.2741	334.81	31.75	2.816	0.318	259.71	(2,1,1)
31.11	2.873	0.6148	149.05	32.15	2.781	0.4203	196.71	(1,1,2)
32.91	2.720	0.4001	230.06	32.87	2.722	0.4856	170.55	(3,0,0)

Small differences in Mg-Zn-CHAp diffractogram compared with Sr-Zn-CHAp can be observed. As can be seen from Table 1, all the peaks determined for Mg-Zn-CHAp were slightly shifted to right compared to Sr-Zn-CHAp, due to the higher ionic radius of the strontium compared to magnesium. In case of Mg-Zn-CHAp most of the calculated crystallite sizes, at different Miller indexes, presented values smaller with 8-75 Å than Sr-Zn-CHAp, as expected. The presence of Mg^{2+} and Zn^{2+} into the apatite structure leads to structural changes in (1,0,2) and (1,1,2) plans, in these cases L being with 38-48 Å higher.

The lattice parameters (a and c) were determined for the (hkl) peaks position from XRD pattern of Mg-Zn-CHAp, specific for the apatite hexagonal crystal structure, based in the inter-planar distance and Miller indexes, according to equation (*6*) and the obtained values are presented in Table 2. The results were compared with hydroxyapatite parameters.

$$\frac{1}{d^2} = \frac{4}{3} \cdot \frac{h^2+hk+k^2}{a^2} + \frac{l^2}{c^2} \qquad (6)$$

Table 2. The a and c lattice parameters and the cell volume for carbonated hydroxyapatite double substituted

Samples	a [Å]	c [Å]	Unit cell volume [Å^3]
Sr-Zn-CHAp [20]	9.4328	6.902	531.6
Mg-Zn-CHAp	9.4271	6.8929	530.5

The substitutions of metallic ions into carbonated hydroxyapatite determined the increase in both a and c lattice parameters in comparison with the standard hydroxyapatite (a=9.4180 Å and c=6.8840 Å) [27]. The changes in lattice dimensional characteristics, as expected, leads to a more extensive unit cell compared with HAp (528.80 Å^3). From Table 2 it can be seen that the Sr-Zn-CHAp sample showed the expansion of both a and c network parameters, and thus a higher cell volume compared to carbonate hydroxyapatite substituted with magnesium and zinc ions. A possible explanation would be the incorporation of a bivalent metallic ions with higher ionic radius than Ca^{2+}, such as strontium (1.12 Å). In the case of the Mg-Zn-CHAp sample, the lower ionic radius of magnesium (0.72 Å) compared to Ca^{2+} (0.99 Å) causes a contraction of the values of the lattice parameters [28]. The metal ions (Sr, Ag, Ba, Zn, K) introduction in the carbonated hydroxyapatite lattice showed an increase in lattice parameters, except Zn^{2+}, which has a smaller ionic radius (0.74 Å) than Ca^{2+} [19]. Addition of Zn into HAp structure can lead also to a decrease of the lattice parameters [29, 30].

SEM micrographs achieved for Mg-Zn-CHAp are presented in Figure 3. Spherical particles of about 200-400 nm can be observed, in comparison with Sr-Zn-CHAp that consists in particles of 700-800 nm. The tendency to agglomerate can be observed also for this sample, when the small size particles form a only a few clusters with diameters varying from 7 to 90 μm, compared with Sr-Zn-CHAp. EDS analysis confirms calcium substitution with Mg and Zn metallic ions.

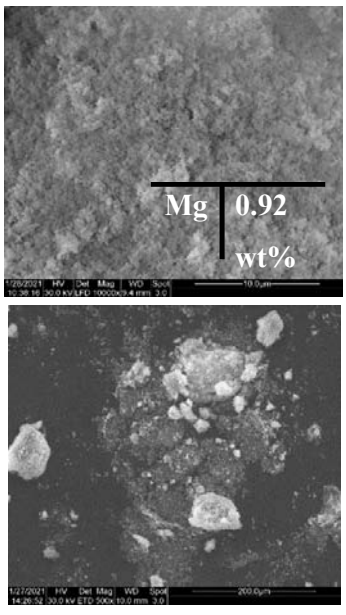

Figure 3. SEM-EDS results for Mg-Zn-CHAp

The two types of double substituted carbonated hydroxyapatite, after synthesis and characterization,

were used as consolidants. In order to study the effect of the inorganic compounds in various methods applied in conservation-restoration procedures, young and 30-years old fir wood specimens were used.

A main characteristic of the consolidated object is considered to be the change in color produced during treatment. Thus, chromatic parameters were determined after the YF and 30F were treated by brushing with the three considered concentrations. The values of the change in L, a, and b parameters compared with the untreated are presented in Table 3.

Table 3. Chromatic Parameters for YF and 30F treated with 0.1g/L, 0.25g/L, 0.5g/L Mg-Zn-CHAp and Sr-Zn-CHAp

Consolidant concentration	YF			30F		
	ΔL	Δa	Δb	ΔL	Δa	Δb
0.1g/L Mg-Zn-CHAp	0.35	0.03	0.51	1.53	0.16	0.50
0.25g/L Mg-Zn-CHAp	0.51	0.13	0.77	3.71	0.24	2.19
0.5g/L Mg-Zn-CHAp	0.96	0.27	0.85	4.78	0.26	2.33
0.1g/L Sr-Zn-CHAp	0.17	0.04	0.28	2.80	0.16	1.18
0.25g/L Sr-Zn-CHAp	0.86	0.24	0.71	3.88	0.22	2.08
0.5g/L Sr-Zn-CHAp	0.90	0.26	1.25	4.94	0.34	2.44

Fir wood is a softwood and it is characterized by: YF: lightness 82.94, green-red (a) values of 4.77, and blue-yellow (b) values of 20.41; 30F: L=58.98; a=3.99; b=9.79. For the samples based on young wood, the highest change in color in observed for a and b variations, and for 30F specimens the main increase was observed for lightness. The color variation of treated aged wood was previously observed [3, 31]. Thus, the young wood has a lighter color appearance.

The increase in lightness, redness and yellowness determined on the treated fir wood samples is produced by increasing the white consolidant concentration. Similar results are obtained for two double substituted carbonated hydroxyapatite applied on wood.

Three classes of stability can be considered in color variation, by analyzing the change in yellowness: if Δb is smaller than 3, the treatment is stable, if the variation has a value between 3 and 8 a moderate stability is obtained, and if the wood difference in color is higher than 8 unstable treatment results. For both types of treated wood, the value of Δb reported to the control samples indicated a high stability of color, making the products suitable for applying on young and old wood objects, in concentration of up to 0.5 g/L.

The total color variation, as presented in Figure 4, has increased values depending of the wood type and consolidant concentration. As expected, for old wood, the color change is more accentuate.

The traditional hammer test for wood is a tools to compare the applied impact speed with the obtain rebound and measures the amount of energy that can be recovered. Thus, the mechanical properties of wood result as compressive strength.

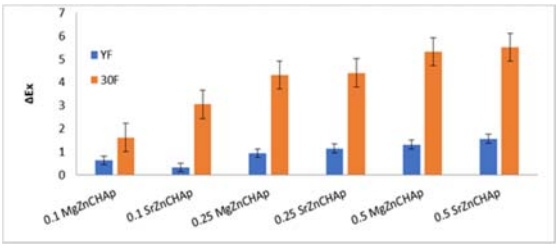

Figure 4. The total color variation of treated wood specimens compared with the control samples

The rebound number was measured for YF and 30F, the samples untreated and treated with double substituted carbonated hydroxyapatite according to ASTM C805 and the variation is presented in Figure 5.

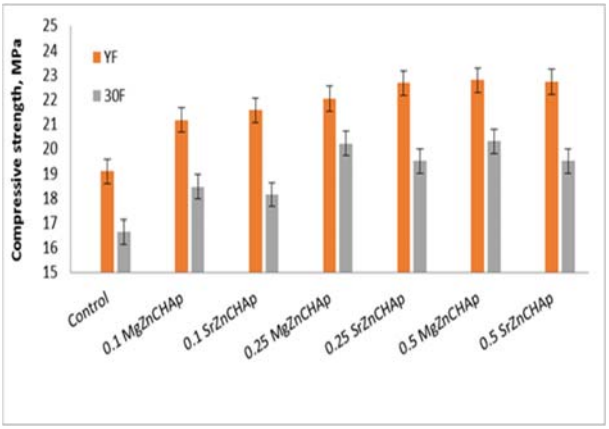

Figure 5. Mechanical strength for control and treated young and 30-years old wood specimens

A slight increase in the strength of the samples can be observed after the application of consolidants, samples presented higher compressive strength values. The young wood appears more rigid and tougher than the old wood because of its stable physical behavior and relatively constant cell size.

Wood has a hydrophilic nature and adsorbs the environmental moisture when it is exposed to real conditions. With a high spread in the European forests, fir wood is a soft wood with a rapid growth that is uniformly textured and has a very low resistance to rot and decay and very used in various applications, including constructions, furniture etc. It presents a straight and uniform fiber, a homogeneous whitish color, which turns into a darker shade in the circle of the interior rings. Its processing is easy due the lack of structural defects like knots. For any outdoor application, it is necessary to apply appropriate treatments to the fir wood, consolidants that can protect the wood and prevent the action of aggressive agents.

One of the important characteristic of wood consist in the ability to absorb and desorb water from and to the environment; the same amount of moisture that enter and exit the wood structure leads to cellular deformation; the way to obtain information regarding this process of sorption-desorption of humidity is to determine the hysteresis index. This phenomenon implies the tensions

and deformations from the wood structure due to the water penetration at molecular and capillary degree.

In real conditions, wood suffer many sorption cycles and high moisture is a good environment for fungi degradation. So, the prediction of the climatic behavior can predict mold and rot development or the wood cracking.

The sorption-desorption curves of control and treated young and 30-years old fir wood samples are presented in Figure 6 and 7. The hysteresis index (HI) calculated for all the samples is also presented in Figure 8, in comparison with the water absorption.

The hysteresis curves indicated less water maintenance into wood capillaries after absorption for 30-years old fir wood. The process is dependent on the previous exposure of the samples to environmental humidity. The sorption process is similar to desorption for all the samples and an improvement of desorption path is evidenced for the specimens treated with 0.25g/L double substituted CHAp.

The curves are similar in form for all the samples, but consolidants action is highlighted by graphic representation of the hysteresis index (HI). A decrease of HI value can be observed for all the treated samples, more pronounced for the 30-years old wood, due to the fact that the rehydrating of the sorption site occurs slowly, the water molecules penetrate less the cell structure of wood and fewer nonopores are formed. Thus, the less amount of hydroxyl sorption sites is available to attach the water molecules. The smaller HI, as previous mentioned, was obtained for the samples treated with 0.25g/L CHAp. Lower HI with up to 20% compared to control can be observed.

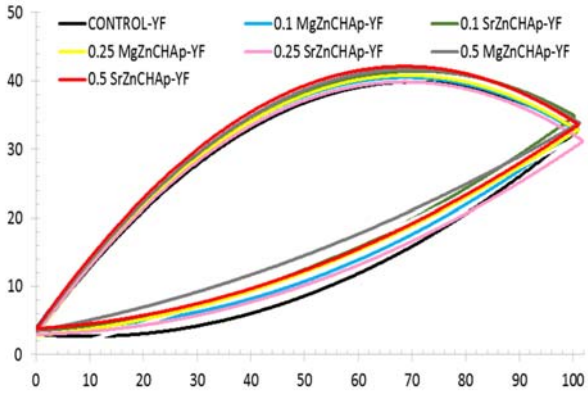

Figure 6. Sorption-desorption curves for control and treated young fir wood specimens

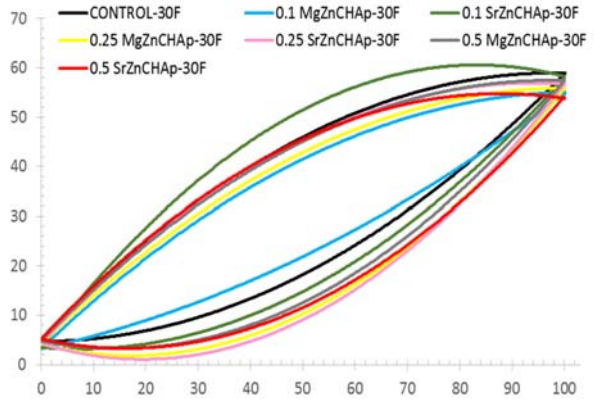

Figure 7. Sorption-desorption curves for control and treated 30-years old fir wood specimens

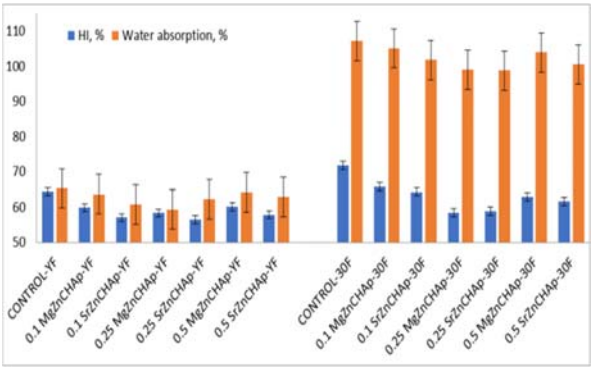

Figure 8. The correlation between the hysteresis index (HI) and the water absorption of fir wood specimens

For the 30-years old wood specimens the equilibrium humidity at hysteresis has higher values for all the samples, the dry nature leading to the absorption of more water into the capillary structure, the high levels of humidity having the ability to plasticize the polymeric components of wood (cellulose, hemicelluloses and lignin), enabling the relaxation of their macromolecular chains. This process leads at the formation of nanopores where water penetrate and can be maintained. Dilatation and contraction of specimens was the result of forming the morphological defects (Figure 9).

The capacity to penetrate into the wood channels and thus to preserve it is shown also by the specimens water absorption, the percentage being in accordance with the HI variation.

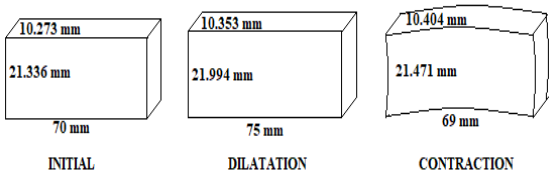

Figure 9. Dimensional changes during sorption-desorption process on the 30-years old wood specimens

5. CONCLUSIONS

Double substituted carbonated hydroxyapatites using Zn^{2+} and Mg^{2+} ions were synthetized using the method previous published for Sr-Zn-CHAp. The presence of the metallic ions was evidenced by FTIR based on both the specific absorption bands for hydroxyapatite structure and the peaks from the 600-400 cm^{-1} range.

Based on XRD diffractograms, changes in apatite structure produced by the inclusion of bivalent metallic ions with different ionic radius than Ca^{2+} are evidenced. Calcium substitution with Mg and Zn metallic ions was also evidenced by EDS. The obtained spherical particles dispersed in water at different concentrations was applied by brushing on young and old fir wood and tested as consolidants.

The efficiency was demonstrated by colorimetry, mechanical testing, water absorption and hysteresis behavior. Small differences in lightness, redness and yellowness and improved mechanical strength, higher for the young wood, were observed on treated wood specimens compared to control.

The hysteresis curves indicated less water maintained into wood capillaries for 30-years old fir wood. For all the samples, the sorption process is similar to desorption for all the samples and an improvement of desorption path was evidenced for the specimens treated with a medium concentration of double substituted CHAp. The hysteresis index presented lower values for all the treated samples, more pronounced for the 30-years old wood, due to the fact that the rehydrating of the sorption site occurs slowly, the water molecules penetrate less the cell structure of wood and fewer nonopores are formed, in accordance with the water absorption.

Acknowledgements: This work was supported by Romanian Ministery of Research and Innovation, CCCDI – UEFISCDI, by grant number 51PCCDI/2018 and by the contract 567 PED/2020.

REFERENCES

[1] Williams RS, Weathering of wood. Handbook of wood chemistry and wood composites, 2005; 7: 139-185.

[2] Laks P, and Heiden PA, Compositions and methods for wood preservation. 2003; U.S. Patent No. 6,521,288 Washington, DC: U.S. Patent and Trademark Office.

[3] Ion RM, Nyokong T, Nwahara N, Suica-Bunghez IR, Iancu L, Teodorescu S, et al. Wood preservation with gold hydroxyapatite system, Heritage Science. 2018; 6(1): 1-12.

[4] Richardson B, Wood Preservation. 2002: Routledge.

[5] Chen F, Gong AS, Zhu M, Chen G, Lacey SD, Jiang F, Li Y, Wang Y, Dai J, Yao Y, Mesoporous, three-dimensional wood membrane decorated with nanoparticles for highly efficient water treatment. Acs Nano, 2017; 11(4): 4275-4282.

[6] Alfieri P, Lofeudo R, and Canosa G, Impregnant formulation to the preservation, protection and consolidation of wood heritage assets, International Journal of Conservation Science, 2018; 9(4): 629-640.

[7] Nicholas DD, Wood Deterioration and Its Prevention by Preservative Treatments: Volume 1: Degradation and Protection of Wood, 1982; Syracuse University Press.

[8] González-Laredo R. F., Rosales-Castro M., Rocha-Guzmán N. E., Gallegos-Infante J. A., Moreno-Jiménez M. R., Karchesy J. J. Wood preservation using natural products. Madera y bosques, 2015; 21(SPE), 63-76.

[9] Pinto APF, and Rodrigues JD, Consolidation of carbonate stones: Influence of treatment procedures on the strengthening action of consolidants. Journal of cultural Heritage, 2012; 13(2): 154-166.

[10] Pinto AF, and Rodrigues JD, Stone consolidation: The role of treatment procedures. Journal of Cultural Heritage, 2008; 9(1): 38-53.

[11] Salazar-Hernández C, Cervantes J, Puy-Alquiza MJ, and Miranda R, Conservation of building materials of historic monuments using a hybrid formulation. Journal of cultural Heritage, 2015; 16(2): 185-191.

[12] Toniolo L, Poli T, Castelvetro V, Manariti A, Chiantore O, and Lazzari M, Tailoring new fluorinated acrylic copolymers as protective coatings for marble. Journal of cultural Heritage, 2002; 3(4): 309-316.

[13] David ME, Ion RM, Andrei ER, Grigorescu RM, Iancu L, and Filipescu MI, Superhydrophobic Coatings Based On Cellulose Acetate For Pinewood Preservation. Journal of Science and Arts, 2020; 1: 171-182.

[14] Simpson WT, Drying and control of moisture content and dimensional changes. Wood handbook: wood as an engineering material. Madison, WI: USDA Forest Service, Forest Products Laboratory, 1999; General technical report FPL; GTR-113: Pages 12.1-12.20, 1999. 113.

[15] Baglioni P, Giorgi R, Soft and hard nanomaterials for restoration and conservation of cultural heritage. Soft Matter, 2006; 2(4): 293-303.

[16] Singh J, Singh H, Magnesium Doped Hydroxyapatite: Synthesis, Characterization and Bioactivity Evaluation. Biomaterials Science: Processing, Properties, and Applications V: Ceramic Transactions; Narayan R, Bose S, Bandyopadhyay A, Eds 2015; 254: 161-174.

[17] Prekajski M, Jokic B, Kalijadis A, Maletaskic J, Stanković N, Luković J, Matovic B, Synthesis of silver doped hydroxyapatite nanospheres using Ouzo effect. Processing and Application of Ceramics, 2016; 10(3): 169-174.

[18] Fahami A, Nasiri-Tabrizi B, Beall G, Moslemzadeh Tehrani P, Basirun W, A top-down approach for the synthesis of nano-sized Ba-doped hydroxyapatite. Journal of the Australian Ceramic Society, 2017; 53(2), 491-498.

[19] Ion RM, Iancu L, Vasilievici G, Grigore ME, Andrei RE, Radu GI, Grigorescu RM, Teodorescu S, Bucurica IA, and Ion ML, Ion-substituted carbonated hydroxyapatite coatings for model stone samples. Coatings, 2019; 9(4): p. 231.

[20] Iancu L, Ion RM, Grigorescu RM, David ME, Ghiurea M, Vasilievici G, Stirbescu RM, and Dulama ID, Double substituted carbonated hydroxyapatite for stone

consolidation. Journal of Science and Arts, 2020; 20(3): 713-730.

[21] Havrlik M, and Ryparová P, Protection of wooden materials against biological attack by using nanotechnology. Acta Polytechnica, 2015; 55(2): 101-108.

[22] EN, U., 15886. Conservation of cultural property. Test methods. Colour measurements of surfaces, 2010.

[23] ASTM D. 2244. Standard Practice for Calculation of Color Tolerances and Color Differences from Instrumentally Measured Color Coordinates. USA; 2013.

[24] Koutsopoulos S, Synthesis and characterization of hydroxyapatite crystals: a review study on the analytical methods. Journal of Biomedical Materials Research: An Official Journal of The Society for Biomaterials, The Japanese Society for Biomaterials, and The Australian Society for Biomaterials and the Korean Society for Biomaterials, 2002; 62(4): 600-612.

[25] Rashad M, Pan FS, Tang A, Asif M, She J, Gou J, Mao J, and Hu H, Development of magnesium-graphene nanoplatelets composite. Journal of composite materials, 2014; 49 (3), 285-293.

[26] Tavares D, Resende C, Quitan MP, Castro LO, Granjeiro J, and Soares GA, Incorporation of strontium up to 5 Mol. (%) to hydroxyapatite did not affect its cytocompatibility. Materials Research, 2011; 14: 456-460.

[27] Ezekiel I, Kasim SR, Ismail YMB, and Noor AFM, Nanoemulsion synthesis of carbonated hydroxyapatite nanopowders: Effect of variant CO32−/PO43− molar ratios on phase, morphology, and bioactivity. Ceramics International, 2018; 44(11): 13082-13089.

[28] Ren F, Leng Y, Xin R, and Ge X, Synthesis, characterization and ab initio simulation of magnesium-substituted hydroxyapatite. Acta Biomaterialia, 2010. 6(7): 2787-2796.

[29] Ren F, Xin R, Ge X, and Leng Y, Characterization and structural analysis of zinc-substituted hydroxyapatites. Acta Biomaterialia, 2009; 5(8): 3141-3149.

[30] Xiao X, Liu R, Chen C, and Huang L, Structural characterization of zinc-substituted hydroxyapatite prepared by hydrothermal method. Journal of materials science: Materials in medicine, 2008. 19(2): 797-803.

[31] Rowell R, Ibach R, McSweeny J, and Nilsson T, Understanding decay resistance, dimensional stability and strength changes in heat-treated and acetylated wood. European Conference on Wood Modification, 4.1-2 (2009): 14-22.